Northumbria Research Link

Citation: Guo, Yuanjun, Zhao, Chao, Zhou, X. S., Li, Yifan, Zu, Xiao-Tao, Gibson, Desmond and Fu, Yong Qing (2015) Ultraviolet sensing based on nanostructured ZnO/Si surface acoustic wave devices. Smart Materials and Structures, 24 (12). p. 125015. ISSN 0964-1726

Published by: IOP Publishing

URL: http://dx.doi.org/10.1088/0964-1726/24/12/125015 <http://dx.doi.org/10.1088/0964-1726/24/12/125015>

This version was downloaded from Northumbria Research Link: http://nrl.northumbria.ac.uk/24772/

Northumbria University has developed Northumbria Research Link (NRL) to enable users to access the University's research output. Copyright © and moral rights for items on NRL are retained by the individual author(s) and/or other copyright owners. Single copies of full items can be reproduced, displayed or performed, and given to third parties in any format or medium for personal research or study, educational, or not-for-profit purposes without prior permission or charge, provided the authors, title and full bibliographic details are given, as well as a hyperlink and/or URL to the original metadata page. The content must not be changed in any way. Full items must not be sold commercially in any format or medium without formal permission of the copyright holder. The full policy is available online: http://nrl.northumbria.ac.uk/policies.html

This document may differ from the final, published version of the research and has been made available online in accordance with publisher policies. To read and/or cite from the published version of the research, please visit the publisher's website (a subscription may be required.)

UniversityLibrary

Northumbria
University
NEWCASTLE

Ultraviolet sensing based on nanostructured ZnO/Si surface acoustic wave devices

Y. J. Guo[1,2], C. Zhao[2], X. S. Zhou[3,2], Y. Li[2], X. T. Zu[1] D. Gibson,[4] and Y. Q. Fu[2]

[1]School of Physical Electronics, University of Electronic Science and Technology of China, Chengdu, 610054, P. R. China

[2] Faculty of Engineering & Environment, University of Northumbria, Newcastle upon Tyne, NE1 8ST, UK

[3] Institute of Nuclear Physics and Chemistry, China Academy of Engineering Physics, Mianyang, 621900, China

4 Institute of Thin Films, Sensors & Imaging, University of the West of Scotland, Paisley PA1 2BE, UK

Corresponding authors: Dr. Yuanjun Guo; E-mail: yuanjun_guo@hotmail.com; and Dr. Richard Fu; Richard.fu@uws.ac.uk

Abstract: Ultraviolet (UV) sensor based on nanostructured ZnO/Si Surface Acoustic Wave (SAW) devices is studied in this paper. The ZnO films sputtered onto Si (100) substrate showed a preferred (0002) orientation and good photoluminescence emission. For the SAW device with a wavelength of 64 μm, a frequency downshift of ~ 1.4 kHz was observed at the Rayleigh mode under a UV light intensity of 0.6 mW/cm^2, whereas the frequency downshift for the Rayleigh mode was increased to

8.3 kHz after integrating ZnO nanorods (NRs) in the ZnO/Si SAW devices. For the SAW device with a wavelength of 20 μm irradiated under a UV light intensity of 0.6 mW/cm^2, a frequency downshift of 25 kHz for the Sezawa mode was obtained compared to a shift of 12 kHz for the Rayleigh mode. After depositing ZnO NRs, the resonant frequency for the Rayleigh mode was increased to 27.4 kHz under the same UV intensity illumination, due to the significant increase in surface-to-volume ratio.

Keywords: SAW device, UV detector, ZnO, Sezawa mode, nanorods

1. Introduction

Ultraviolet (UV) sensors are widely used in various fields, such as flame detection [1] (fire alarm systems, missile plume detection, and combustion engine control), biological and chemical processes (ozone detection, determination of pollution levels in air, biological agents detection) [2, 3] and aerospace/ astronomy [4, 5] (early missile plume detection, secure space-to-space communications, intra- and inter-satellite communications), etc. For UV sensing applications, surface acoustic wave (SAW) sensors offer many attractive features including fast response, easy reproducibility, high sensitivity, wireless and remote sensing capability [6, 7]. In a SAW sensor, changes of wave frequency (velocity), amplitude (attenuation) and phase are caused by perturbations in the wave propagation, for example, acoustoelectric interactions or mass loading effects [8-10]. Acoustoelectric interactions on the surface

of a piezoelectric material can be utilized effectively for light-sensing applications when the surface of a piezoelectric materail is coated with a suitable optical active overlayer, so that the photogenerated carriers can effectively interact with the piezoelectric fields, causing changes in the frequency or phase [8].

Zinc oxide (ZnO) has been frequently applied in UV sensors due to its attractive optical properties, including its band gap of 3.4 eV and a large exciton binding energy of 60 meV at room temperature [11]. ZnO has been deposited onto various piezoelecric materials for fabricating UV detectors based on SAW devices, such as ZnO/sapphire [12], ZnO/quartz [13], ZnO/$LiNbO_3$ [14] and ZnO/$LiTaO_3$ [15]. However, these substrates are relatively expensive or fragile, and are less compatible with semiconductor manufacturing process for integrated control and signal processing electronics. In order to enhance the operating frequency of the SAW device, thereby improving its sensitivity, many researchers have used high acoustic velocity substrate materilas (such as diamond) or an advanced lithography process (such as e-beam or deep-UV lithography) to produce interdigital transducers (IDTs) with sub-micron finger widths [16]. However, these methods result in high cost SAW devices or a complex fabrication process. Recently, there has been an increased interest in using ZnO itself as a high performance piezoelectric thin film materials in SAW based sensing devices [17-19]. Using the ZnO thin film as a SAW substrate, rather than brittle or expensive bulk materials of $LiNbO_3$ or quartz, it is compatible with integrating microelectronics, multiple sensing incorporation or microfluidics

techniques for a lab-on-chip with low cost and multi-functions on various substrates (silicon, glass or polymer) [20].

As the sensitivity of the SAW devices is improved with increased wave frequency, using the higher mode (such as Sezawa mode) waves or higher harmonic modes of the fundamental waves, should provide a better performance for UV sensing [21]. For thin film SAW devices based on ZnO or AlN films, with increasing film thickness, a higher frequency Sezawa wave can be generated above a thickness approximately hk=1 (h is the thickness of the film, and k=2π/λ) [22]. Sezawa mode wave generally has a higher acoustic velocity and propagates more near to the SAW device surface compared with the Rayleigh mode wave, thus could lead to a larger photo-response and a potential larger maximum effective piezoelectric coupling constant [23, 24]. On the other hand, ZnO nanostructures are a potential sensing candidate for UV sensors due to their high surface to volume and large ON/OFF current ratios, fast response and recovery, visible light blind, and low-cost fabrication [25].

Although ZnO-based SAW UV light sensors have been developed and studied, most use the Rayleigh (or fundermental) mode for sensing or only use ZnO film as the UV sensing material [13, 14, 21, 26, 27]. In addition, many UV sensors based on ZnO nanostructures as the sensing material have been reported, however, most of them are characterized by current–voltage measurement, not based on SAW measurment [25, 28-30]. In this work, we investigate two ways to improve the UV sensing response based on ZnO/Si SAW devices: one using Sezawa mode instead of Rayleigh mode, and the other using ZnO NRs instead of ZnO film as the sensing material.

2. Experimental details

ZnO films of ~4.5 μm thick were deposited on four-inch silicon (100) substrate using a standard DC magnetron sputtering from a Zn (99.99%) target at a power of 400 W and Ar/O_2 flow ratio of 50/45 SCCM (standard cubic centimetre per minute) without separate substrate heating. During deposition the gas pressure was ~5 mTorr. The bi-directional aluminium interdigitated transducers (IDTs) with a thickness 150 nm were patterned onto the ZnO/Si substrates using a standard photolithography process. The SAW IDTs were designed with 60 pairs of finger electrodes and an aperture of 5 mm, with wavelengths of 20 and 64 μm. The distance between two opposite IDTs was 5 mm.

ZnO NRs were prepared to be integrated into the ZnO/Si SAW devices to enhance the sensing performance. Figure 1(a) shows the schematic layered structure of ZnO/Si with ZnO NRs. On the ZnO/Si SAW devices and between two opposite IDTs, a 20 nm TiO_2 insulating layer was deposited using DC magnetron sputtering with a power of 550 W, Ar/O_2 gas flow rates of 4.5/4.5 SCCM and a pressure of ~4.5 mTorr. The reason for adding this TiO_2 layer is to separate the bulk ZnO film from the seed layer of ZnO NRs growth. On top of this TiO_2 layer, a 50 nm ZnO seed layer was prepared using DC magnetron sputtering, with the same deposition condition as that for the ZnO film. ZnO NRs were then grown on top of the ZnO seed layer using a hydrothermal method [31]. In a typical synthesis, the precursor solution containing

equal molar zinc nitrate hexahydrate ($Zn(NO_3)_2 \cdot 6H_2O$, Sigma-Aldrich, ≥99.0 % purity) and methenamine ($C_6H_{12}N_4$, HMTA, Sigma-Aldrich, ≥99.0 % purity) was added into a sealed container. The ZnO/Si SAW device was suspended upside-down in the precursor solution. The device was kept in the solution of 50 mM at 90 ^oC for 3 hours. After growth the device was taken out and rinsed with deionized water to remove the surface residues.

Cross-section and surface morphology of ZnO film and NRs was characterized using scanning electron microscopy (SEM, Hitachi S4100). Crystalline structures of both the ZnO films and NRs were studied using X-ray diffraction (XRD, Siemens D-5000 diffractometer, Cu Kα, λ=0.154 nm). Photoluminescence (PL) spectra of both the ZnO film and NRs were measured at room temperature using a fluorescence spectrometer (LS-55, Perkin-Elmer Xe-lamp excitation at 325 nm and room temperature).

Resonant frequency and ZnO SAW device performance were characterized using an HP8752A network analyzer. The UV sensing was performed by illuminating the SAW devices (mounted on a bulk aluminum black) with a 365 nm UV source (Sylvania F8W/BLB-T5). The output power density of the UV source was measured using a photometer (EALING corporation U.S.A). The shift of SAW device resonant frequencies under UV irridation were characterized using an HP8752A network analyzer, data acquisition by a LabVIEW based software with the computer control

system. In the test, all of the device characterizations and UV light detections were conducted at room temperature. The temperature was monitored during UV light exposure, and no significant temperature rise was observed.

3. Results and discussion

3.1. ZnO film and SAW device characterization

Figure 1(b) shows cross-section SEM images of ZnO NRs/ZnO/Si structure, in which the ZnO seed layer and TiO_2 insulate layer are too thin to be visible. The ZnO film has dense nano-columnar structures. Figure 1(c) shows top-view of the ZnO NRs. The ZnO NRs are densely packed and the diameters and lengths of ZnO NRs are estimated to be 50-150 nm and 1.1-1.3 μm, respectively.

XRD results of the ZnO/Si structure are shown in figure 2(a) and confirm the preferred (0002) orientation or *c*-axis growth for both the ZnO film and NRs (with a peak at 2θ=34. 12^o and 34.14^o for ZnO film and NRs, respectively). The peak position of ZnO NRs shifts to the right with the angle of 0.02^o compared with that of ZnO film, which has large compressive film stress.

The measured PL spectra of the ZnO/Si structure at room temperature are shown in figure 2(b). For both ZnO film and NRs, two emission bands were observed, i.e., one is the UV near-band-edge emission and the other is the visible emission which was

commonly associated with the deep-level emission. The dominant UV emission at 389 and 390 nm can be assigned to the exciton recombination, which suggestes that the ZnO film and NRs possess a good crystallinity [32]. A few weak emission peaks in the region between 420 and 540 nm were also detected, which are attributed to the presence of point defects such as oxygen vacancies and zinc interstitials [33, 34]. The presence of the defects indicates that the ZnO film and NRs are slightly oxygen-deficeient. Besides, the intensity of UV emission at 390 nm for ZnO NRs is higher than that for ZnO film. For ZnO film, the absorption coefficient at 365 nm is about (10^4–10^5 cm^{-1}) [35]. Due to a larger surface-to-volume ratio of the ZnO NRs, more UV light will be absorbed and more excitons will appear under UV light illumination, which will lead to a higher UV near-band-edge emission.

For the ZnO/Si structure with a wavelength of 64 μm (corresponding to hk=0.44, in which h is the thickness of the film, and k=2π/λ), Rayleigh mode with the resonant peak at 63.20 MHz was detected as shown in figure 3(a). The calculated phase velocity of the Rayleigh wave is 4045 m/s. After growth of the ZnO NRs on top of the SAW structure, the resonant frequency of Rayleigh mode was decreased to 59.75 MHz, and the calculated phase velocity becomes 3824 m/s.

For the SAW device with a wavelength of 20 μm (corresponding to hk=1.4), two resonant peaks at 180.71 MHz and 271.83 MHz were observed as shown in figure 3(b) and (c), corresponding to the Rayleigh wave and Sezawa wave, respectively. The

calculated phase velocities of the Rayleigh wave and Sezawa wave are 3614 and 5437 m/s, respectively. After growth of the ZnO NRs on top of the SAW structure, the resonant frequency of Rayleigh mode was decreased to 174.5 MHz, and the calculated phase velocity is 3490 m/s. Whereas the Sezawa mode frequency was not apparently identified after depositing ZnO NRs.

3.2 UV sensing results

For the SAW device with a wavelength of 20 μm, the changes of the resonant frequency under UV illumination are shown in figure 4. For the Rayleigh wave at the resonant frequency of 180.71 MHz, a frequency downshift of ~ 12 kHz was observed at a UV light intensity of 0.6 mW/cm^2, as shown in figure 4(a). However, under the same UV light intensity, a larger frequency downshift of ~ 25 kHz was observed for the Sezawa mode at the resonant freqreuncy of 271.83 MHz.

To investigate the reproducibility of UV sensing, real-time responses of the frequency of Rayleigh mode and Sezawa mode were recorded. Figure 4(b) shows the results with the UV light source being switched on and off for three cycles. The resonant frequencies decreased rapidly when the 365 nm UV light at a light intensity of 0.6 mW/cm^2 was switched on, and saturated after a transient time. The maximum frequency shifts of Rayleigh mode and Sezawa mode based SAW UV sensor are ~ -12 and -25 kHz, respectively, which were stable with time and repeated illumination. When the UV light was switched off, the resonant frequencies retured to their original

values without apparent deterioration, showing a good reproducibility.

Figure 4(c) shows the frequency shift as a function of UV intensity for Rayleigh mode and Sezawa mode. It is clear that the frequency shifts of both the Rayleigh mode and Sezawa mode increase linearly with UV light intensity in the tested range of 0-0.6 mW/cm^2. Noted that the frequency shift will be saturated at a certain UV intensity which can be attributed to the saturation of photogenerated carriers [27]. As the number of carriers that can be photoexited from valence band to conduction band is finite under UV light illumination, the photogenerated carriers will not increase unlimitedly with the increased intensities of UV light illumination, however saturate at certain UV intensity. The frequency shifts are directly proportional to the number of photogenerated carriers. Therefore, the frequency shift will be saturated at a certain UV intensity.

Figure 4(d) shows the frequency shift of Rayleigh wave for the ZnO/Si SAW device with a wavelength of 20 μm with and without ZnO NRs. Under a 0.6 mW/cm^2 UV light illumination, the resonant frequency shift for the Rayleigh mode is ~ 12 kHz. However, after depositing ZnO NRs on the top of ZnO seed layer, the resonant frequency shift for the Rayleigh mode was about 27.4 kHz under the same UV intensity illumination. As we have showed in the last paragraph, section 3.1, after growth of the ZnO NRs on top of the SAW, the resonant frequency of Rayleigh mode was decreased to 174.5 MHz, whereas the Sezawa mode frequency was not

apparently identified after depositing ZnO NRs.

Figure 5 shows the frequency shift of Rayleigh wave for the ZnO/Si SAW device with a wavelength of 64 μm with and without ZnO NRs. Under a 0.6 mW/cm^2 UV light illumination, the resonant frequency shift for the Rayleigh mode is only ~ 1.4 kHz. However, after depositing ZnO NRs on top of the ZnO seed layer, the resonant frequency for the Rayleigh mode was decreased about 8.3 kHz under the same UV intensity illumination. It is clear that after adding a layer of ZnO NRs, there is a significant increase in the frequency shift for the Rayleigh mode under UV irridiation and the value was increased almost 6 times.

When a SAW propagates along the piezoelectric substrate, static charges are induced at the surface of the piezoelectric substrate by piezoelectric effect with a consequent electrostatic field formed by the induced static charges. Under UV illumination, the incident light is absorbed by semiconducting ZnO to generate electron-hole pairs, which change the produced electrostatic field at the surface of the piezoelectric substrate. This phenomenon causes the propagating SAW to change, such as velocity decreasing and attenuation increase. The interaction between the photon-generated carriers and the propagating SAW is called acoustoelectric effect [8]. The relation between the conductivity of sensing layer and SAW velocity is provided from the following relation [36, 37]:

$$\frac{\Delta V}{V_0} = -\frac{K^2}{2}\frac{1}{1+(\frac{V_0 c_s}{\sigma_s})^2} \quad (1)$$

Where K^2 is the electromechanical coupling coefficien for the device, σ_s is the sheet conductivity of the sensing film, V_0 is the SAW velocity on free surface, and c_s is the capacitance per unit lengh of the SAW device. From equation (1), under UV illumination, the increase in the conductivity of the sensing layer (σ_s) with increased UV light intensity will decrease the SAW velocity, i.e. the resonant frequency. As ZnO NRs sensing layer has a larger specific surface area than the ZnO film, therefore, more UV light was absorbed on the surface of the ZnO NRs than that of the ZnO film under the same UV light illumination, providing more free electron-hole pairs and consequently larger surface conductivity. Thus, the ZnO/Si device with ZnO NRs has a larger frequency shift according to equation (1).

Table 1 shows the comparison of UV light detectors based on SAW devices with ZnO as the sensing material. The UV light sensitivity of the SAW devices is defined as,

$$S_{UV} = \frac{1}{f_r}\frac{\Delta f}{\Delta I_{UV}} \quad (2)$$

Where f_r is the resonace frequency, Δf is the frequency shift of SAW devices, and ΔI_{UV} is the variation of UV light intensity. In this work, for the ZnO/Si SAW device with a wavelength of 20 μm, the UV light sensitivity for the Rayleigh wave is 110.67 ppm $(mW/cm^2)^{-1}$, while it is 153.28 ppm $(mW/cm^2)^{-1}$ for the Sezawa wave. After depositing ZnO NRs, the UV light sensitivity for the Rayleigh wave is 261.70 ppm $(mW/cm^2)^{-1}$, increasing over twice the values of the Rayleigh wave of the device without ZnO NRs. For the ZnO/Si structure with a wavelength of 64 μm, the UV light

sensitivity for the Rayleigh wave is only 36.92 ppm $(mW/cm^2)^{-1}$. However, after depositing ZnO NRs, it became 231.52 ppm $(mW/cm^2)^{-1}$, increasing almost 6 times as much as that for the device without ZnO NRs. Compared with the experimental results listed in references [13], [14] and [21], the UV light sensitivities in this work are compatible, especailly for ZnO NRs, which has the largest sensitivity in Table 1. The different frequency shifts and sensitivity are associated with the differences in UV intensity, growth substrate, conditions for ZnO thin film deposition，SAW mode，intrinsic freqnency, et al. In this work, SEM, XRD and PL results mentioned above show that ZnO film and NRs have high crystal quality and are believed to be responsible for the enhanced SAW device UV light responses and high sensitivity of the sensors. The experiment results in this work demonstrate that using Sezawa wave instead of Rayleigh waves, and using ZnO NRs instead of film itself are beneficial to the improvement of UV light sensitivity.

4. **Conclusion**

In this study, in order to improve the ZnO/Si SAW devices UV sensing response, Sezawa mode has been utilized rather than a Rayleigh mode. Moreover, ZnO NRs has been used instead of ZnO film as the UV sensing material to improve sensitivity. For the SAW device with a wavelength of 64 μm, only a frequency downshift of ~ 1.4 kHz was observed at the Rayleigh mode under the UV light intensity of 0.6 mW/cm^2. After adding a layer of ZnO NRs, the frequency downshift for the Rayleigh mode was

increased ~ 8.3 kHz due to a larger surface-to-volume ratio of the sensing material. For the SAW device with the wavelength of 20 μm, a relative larger frequency downshift of 25 kHz for the Sezawa mode was obtained compared to 12 kHz at the Rayleigh mode under the same UV light intensity of 0.6 mW/cm^2. After depositing ZnO NRs on the top of ZnO seed layer, the resonant frequency for the Rayleigh mode was shifted about 27.4 kHz under the same UV intensity illumination.

Acknowledgment

The authors acknowledge Royal Society of Edinburgh and Royal academy of Engineering-Research Exchange with China and India, the National Natural Science Foundation of China (No. 11304032), as well as EPSRC (Engineering and Physical Sciences Research Council, UK) Engineering Instrument Pool for providing the characterisation facilities.

References

[1] E Munoz, E Monroy, J L Pau, F Calle, F Omnes and P J Gibart 2001 III nitrides and UV detection *Phys.: Condens. Matter.* 13 7115

[2] A Kolmakov and M Moskovits 2004 Chemical sensing and catalysis by one-dimensional metal-oxide nanostructures *Annu. Rev. Mater. Res.* 34 151-80

[3] K Saha, S S Agasti, C Kim, X Li and V M Rotello 2012 Gold nanoparticles in chemical and biological sensing *Chem. Rev.* 112 2739

[4] C L Joseph 1995 UV Image sensors and associated technologies *Exp. Astron.* 6 97-127

[5] R R Meier 1991 Ultraviolet spectroscopy and remote sensing of the upper atmosphere *Space Sci. Rev.* 58 1-185

[6] P Sharma, S Kumaral and K Sreenivas 2003 Interaction of surface acoustic waves and ultraviolet light in ZnO films *J. Mater. Res.*18 545-8

[7] S Y Wang, Z J Li, X S Zhou, X T Zu, Y Q Fu 2015 Advances in Nanostructured Acoustic Wave Technologies for Ultraviolet Sensing *Nanosci. Nanotechnol. Lett.* 7 169-92

[8] V Chivukula, D Ciplys, M Shur and P Dutta 2010 ZnO nanoparticle surface acoustic wave UV sensor *Appl. Phys. Lett.* 96 233512

[9] C Wen, C Zhu, Y Ju, H Xu and Y Qiu 2010 A novel NO_2 gas sensor using dual track SAW device *Sens. Actuat. A* 159 168-73

[10] S K R S Sankaranarayanan, R Singh and V R Bhethanabotla 2010 Acoustic streaming induced elimination of nonspecifically bound proteins from a surface acoustic wave biosensor: Mechanism prediction using fluid-structure interaction

models *J. Appl. Phys.*108 104507

[11] Z K Tang, G K L Wong, P Yu, M Kawasaki, A Ohtomo, H Koinuma and Y Segawa 1998 Room-temperature ultraviolet laser emission from self-assembled ZnO microcrystallite thin films *Appl. Phys. Lett.* 72 3270

[12] N W Emanetoglu, J Zhu, Y Chen, J Zhong, Y Chen and Y Lu 2004 Surface acoustic wave ultraviolet photodetectors using epitaxial ZnO multilayers grown on r-plane sapphire *Appl. Phys. Lett.* 85 3702

[13] S Kumar, G H Kim, K Sreenivas and R P Tandon 2009 ZnO based surface acoustic wave ultraviolet photo sensor *J. Electroceram* 22 198-202

[14] P Sharma and K Sreenivas 2003 Highly sensitive ultraviolet detector based on ZnO/$LiNbO_3$ hybrid surface acoustic wave filter *Appl. Phys. Lett.* 83 3617-9

[15] H F Pang, Y Q Fu, Z J Li, Y F Li, F Placido, A Walton and X T Zu 2013 Love mode surface acoustic wave ultraviolet sensor using ZnO films deposited on 36 ° Y-cut $LiTaO_3$ *Sens. Actuat. A* 193 87-94

[16] S Seo, W Shin and J Park 2002 A novel method of fabricating ZnO/diamond/Si multilayers for surface acoustic wave (SAW) device applications *Thin Solid Films* 416 190-6

[17] Y Q Fu, L Garcia-Gancedo, H F Pang, S Porro, Y W Gu, X T Zu, F Placido, J I B Wilson, A J Flewitt and W I Milne 2012 Microfluidic of ZnO/nanocrystalline diamond surface acoustic wave devices *Biomicrofluidics* 6 013864

[18] Y Q Fu, Y Li, C Zhao, F Placido and A J Walton 2012 Surface acoustic wave nebulization on nanocrystalline ZnO film *Appl. Phys. Lett.* 101 194101

[19] J Zhou, M DeMiguel-Ramos, L Garcia-Gancedo, E Iborra, J Olivares, H Jin, J K Luo, A S Elhady, S R Dong, D M Wang and Y Q Fu 2014 Characterisation of aluminium nitride films and surface acoustic wave devices for microfluidic applications *Sens. Actuat. B* 202 984-92

[20] Y Q Fu, J K Luo, X Y Du, A J Flewitt, Y Li, G H Markx, A J Walton and W I Milne 2010 Recent developments on ZnO films for acoustic wave based bio-sensing and microfluidic applications: a review *Sens. Actuat. B* 143 606-19

[21] D Phan and G Chung 2012 Characteristics of SAW UV sensors based on a ZnO/Si structure using third harmonic mode *Current Applied Physics* 12 210-3

[22] V Panella, G Carlotti, G Socino, L GioVannini, M Eddrief, K Amimer and C Sébenne 1997 Brillouin scattering study of epitaxial InSe films grown on the Si(111)1 ×1–H surface *J. Phys.: Condens. Matter* 9 5575-80

[23] X Y Du, Y Q Fu, S C Tan, J K Luo, A J Flewitt, W I Milne, D S Lee, N M Park, J Park, Y J Choi, S H Kim and S Maeng 2008 ZnO film thickness effect on surface acoustic wave modes and acoustic streaming *Appl. Phys. Lett.*93 094105

[24] N W Emanetoglu, J Zhu, Y Chen, J Zhong, Y Chen and Y Lu 2004 Surface acoustic wave ultraviolet photodetectors using epitaxial ZnO multilayers grown on r-plane sapphire *Appl. Phys. Lett.* 85 3702

[25] M Amin, N A Shah and A S Bhatti 2015 Development of highly sensitive UV sensor using morphology tuned ZnO nanostructures *Appl. Phys. A* 118 595-603

[26] X L He, J Zhou, W B Wang, W P Xuan, X Yang, H Jin and J K Luo 2014 High performance dual-wave mode flexible surface acoustic wave resonators for UV

light sensing *J. Micromech. Microeng.* 24 055014

[27] C Wei, Y Chen, C Cheng, K Kao, D Cheng and P Cheng 2010 Highly sensitive ultraviolet detector using a ZnO/Si layered SAW oscillator *Thin Solid Films* 518 3059-62

[28] K SAXENA, A Kumar, N Malik, P Kumar and V K Jain 2014 Ultraviolet sensing properties of polyvinyl alcohol-coated aluminum-doped zinc oxide nanorods *Bull. Mater. Sci.* 37 295-300

[29] T Rashid, D Phan and G Chung 2013 Effects of electrolyte on ZnO nanostructures synthesized by galvanostatic electrochemical deposition and their UV sensing properties *Current Applied Physics* 13 1316-20

[30] F Fang, J Futter, A Markwitz and J Kennedy 2009 UV and humidity sensing properties of ZnO nanorods prepared by the arc discharge method *Nanotechnology* 20 245502

[31] H S Hong, D T Phan and G S Chung 2012 High-sensitivity humidity sensors with ZnO nanorods based two-port surface acoustic wave delay line *Sens. Actuat. B* 171– 172 1283-7

[32] R Yousefi and B Kamaluddin 2009 Dependence of photoluminescence peaks and ZnO nanowires diameter grown on silicon substrates at different temperatures and orientations *J. Alloy. Comp.*479 11-4

[33] Q Kuang, Z Y Jiang, Z X Xie, S C Lin, Z W Lin, S Y Xie, R B Huang and L S Zheng 2005 Tailoring the Optical Property by a Three-dimensionally Epitaxial Heterostructure: A Case of ZnO/SnO_2 *J. Am. Chem. Soc.* 127 11777

[34] C C Wu, D S Wuu, P R Lin, T N Chen and R H Horng 2009 Three-Step Growth of Well-Aligned ZnO Nanotube Arrays by Self-Catalyzed Metalorganic Chemical Vapor Deposition Method *Cryst. Growth Des.* 9 4555-61

[35] L W Lai and C T Lee 2008 Investigation of optical and electrical properties of ZnO thin films *Mater. Chem. Phys.* 110 393-6

[36] M Penza, P Aversa, G Cassano, W Wlodarski and K Kalantar-zadeh 2007 Layered SAW gas sensor with single-walled carbon nanotube-based nanocomposite coating *Sens. Actuat. B* 127 168-78

[37] Y L Tang, Z J Li, J Y Ma, H Q Su, Y J Guo, L Wang, B Du, J J Chen, W Zhou、Q K Yu, X T Zu 2014 Highly sensitive room-temperature surface acoustic wave (SAW) ammonia sensors based on Co_3O_4/SiO_2 composite films *Journal of Hazardous Materials* 280 127-33

Table 1. Comparison of UV light detectors based on SAW devices.

Detecting layer	Substrate	Resonance mode	Resonance frequency (MHz)	Frequency shift (KHz)	UV intensity (mw/cm^2)	Sensitivity ($ppm\ (mw/cm^2)^{-1}$)
ZnO[a]	Quartz	Rayleigh	41.2	45	19	57.49
ZnO[b]	$LiNbO_3$	Rayleigh	37	170	40	114.87
ZnO[c]	Si	Rayleigh	122.15	10	3	27.29
ZnO[d]	Si	Rayleigh	180.71	12	0.6	110.67
ZnO NRs[d]	Si	Rayleigh	174.5	27.4	0.6	261.70
ZnO[d]	Si	Sezawa	271.83	25	0.6	153.28
ZnO[d]	Si	Rayleigh	63.2	1.4	0.6	36.92
ZnO NRs[d]	Si	Rayleigh	59.75	8.3	0.6	231.52

[a] Reference [13]. [b] Reference [14]. [c] Reference [21]. [d] This work.

FIGURE CAPTIONS

Figure 1. (a) Schematic layered structure of ZnO/Si structure with ZnO NRs. SEM images: (b) cross-section morphology of the composite structure, and (c) surface morphology of the NRs.

Figure 2. Characterization of ZnO/Si and ZnO NRs/ZnO/Si structures: (a) XRD spectra, and (b) PL spectra.

Figure 3. Transmission (S_{21}) spectra of the ZnO/Si devices with a wavelength of 64 μm (a) with and without ZnO NRs; 20 μm: (b) Rayleigh mode, and (c) Sezawa mode.

Figure 4. Frequency shift for the ZnO/Si device with a wavelength of 20 μm with 365 nm UV light illuminated at a power density of 0.6 mW/cm^2: (a) Rayleigh mode and Sezawa mode, and (b) Rayleigh mode and Sezawa mode under a cyclic illumination of the UV light. (c) Frequency shift as a function of UV intensity for Rayleigh mode and Sezawa mode. (d) Frequency shift for Rayleigh mode with and without ZnO NRs with 365 nm UV light illuminated at a power density of 0.6 mW/cm^2.

Figure 5. Frequency shift for Rayleigh mode for the ZnO/Si structure with a wavelength of 64 μm with and without ZnO NRs with 365 nm UV light illuminated at a power density of 0.6 mW/cm^2.

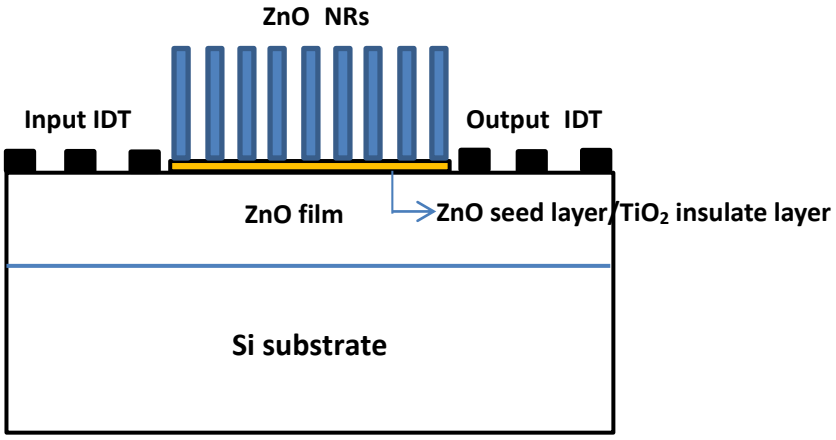
ZnO NRs
Input IDT
Output IDT
ZnO film
ZnO seed layer/TiO2 insulate layer
Si substrate

(a)

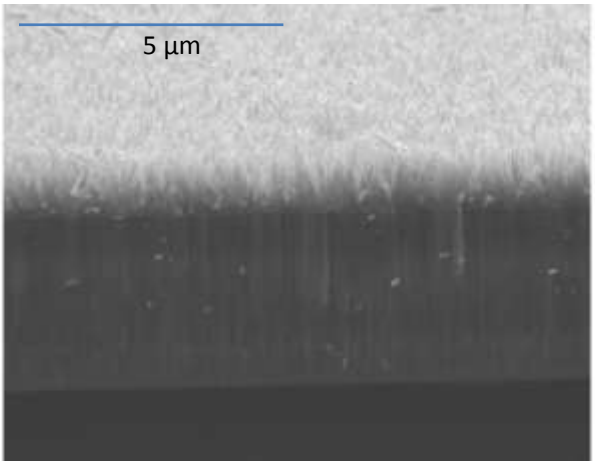
5 μm

(b)

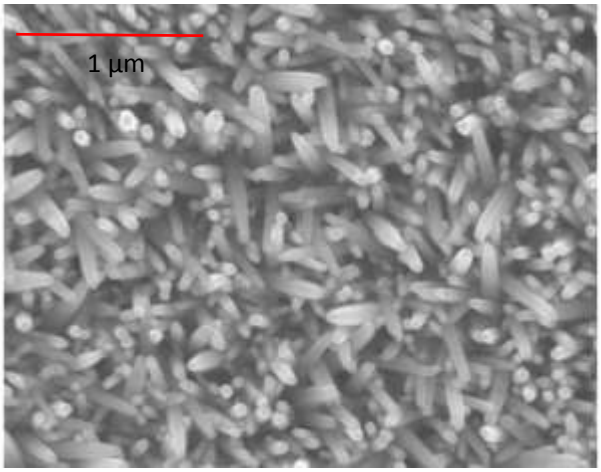
1 μm

(c)

Figure 1.

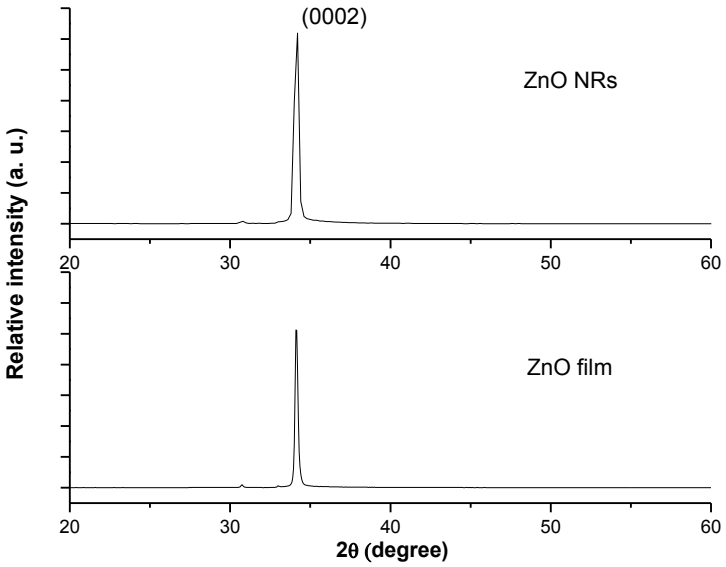
(0002)
ZnO NRs
ZnO film
Relative intensity (a. u.)
20
30
40
50
60
2θ (degree)

(a)

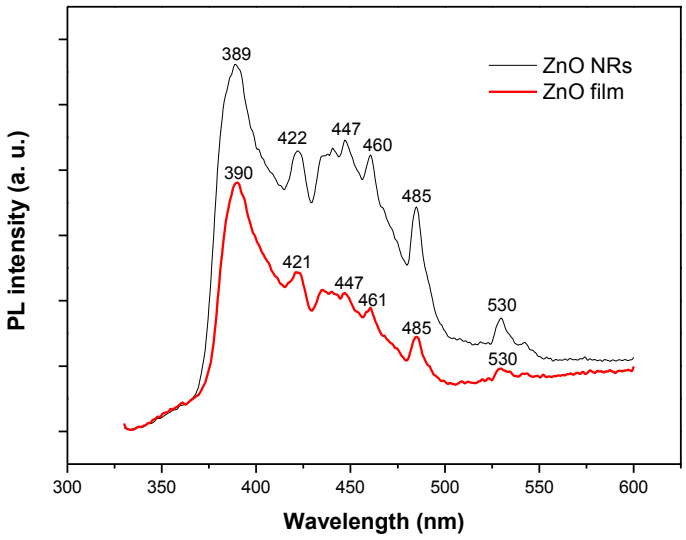
389
422
447
460
485
530
390
421
447
461
485
530
ZnO NRs
ZnO film
PL intensity (a. u.)
300
350
400
450
500
550
600
Wavelength (nm)

(b)

Figure 2.

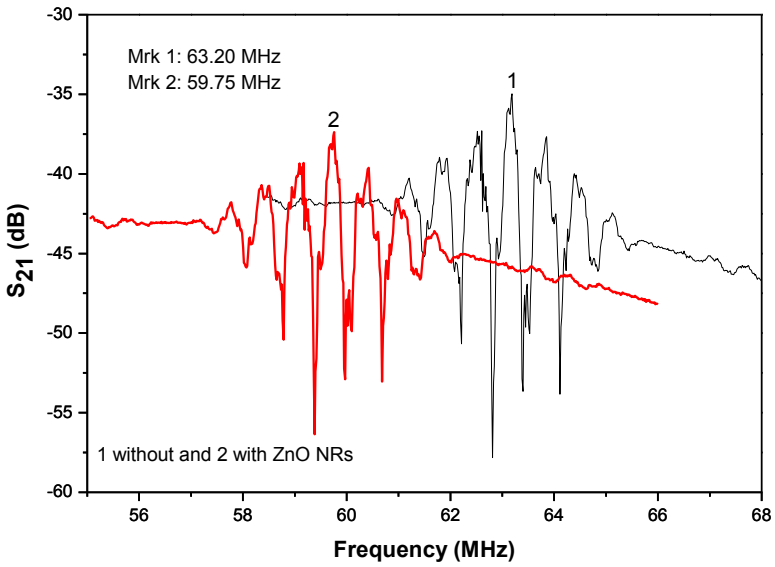
Mrk 1: 63.20 MHz
Mrk 2: 59.75 MHz
1
2
1 without and 2 with ZnO NRs
S21 (dB)
Frequency (MHz)
-30
-35
-40
-45
-50
-55
-60
56
58
60
62
64
66
68

(a)

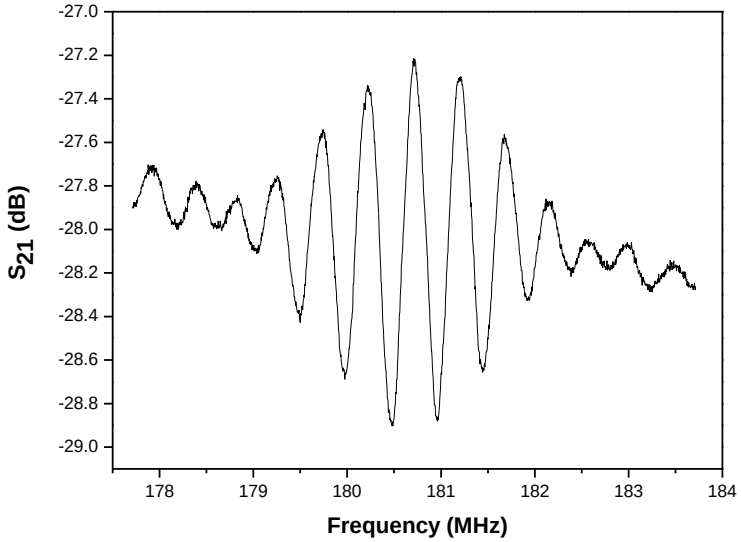
S21 (dB)
Frequency (MHz)
-27.0
-27.2
-27.4
-27.6
-27.8
-28.0
-28.2
-28.4
-28.6
-28.8
-29.0
178
179
180
181
182
183
184

(b)

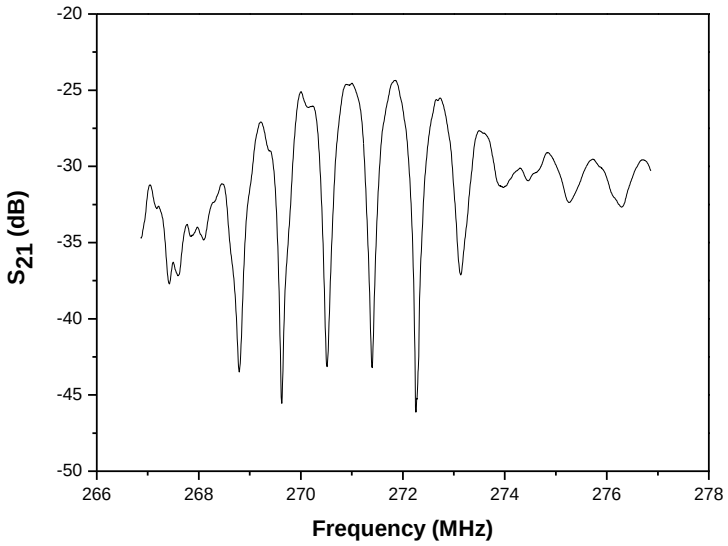
-20
-25
-30
-35
-40
-45
-50
S21 (dB)
266
268
270
272
274
276
278
Frequency (MHz)

(c)

Figure 3.

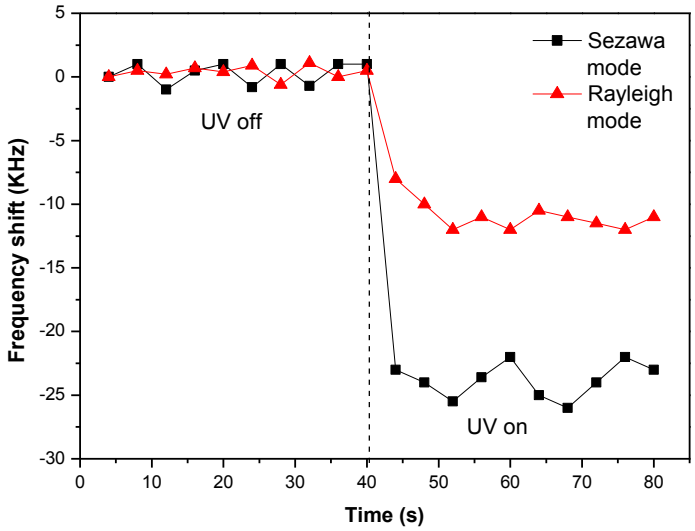
Sezawa mode
Rayleigh mode
UV off
UV on
Frequency shift (KHz)
Time (s)
5
0
-5
-10
-15
-20
-25
-30
0
10
20
30
40
50
60
70
80

(a)

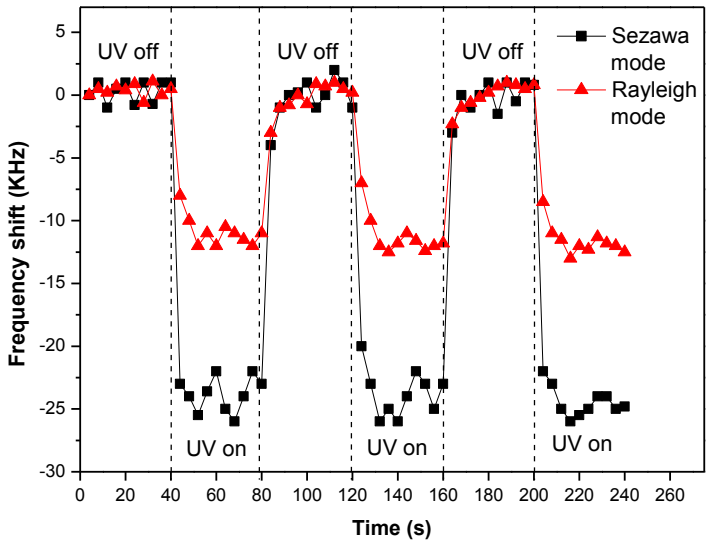
Sezawa mode
Rayleigh mode
UV off
UV off
UV off
UV on
UV on
UV on
Frequency shift (KHz)
Time (s)
5
0
-5
-10
-15
-20
-25
-30
0
20
40
60
80
100
120
140
160
180
200
220
240
260

(b)

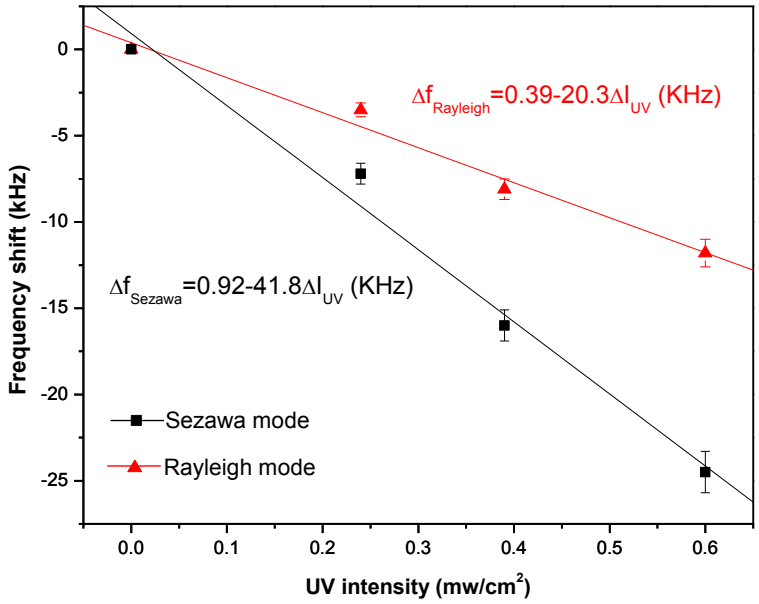
Frequency shift (kHz)
UV intensity (mw/cm^2)
$\Delta f_{Rayleigh}$=0.39-20.3ΔI_{UV} (KHz)
Δf_{Sezawa}=0.92-41.8ΔI_{UV} (KHz)
Sezawa mode
Rayleigh mode

(c)

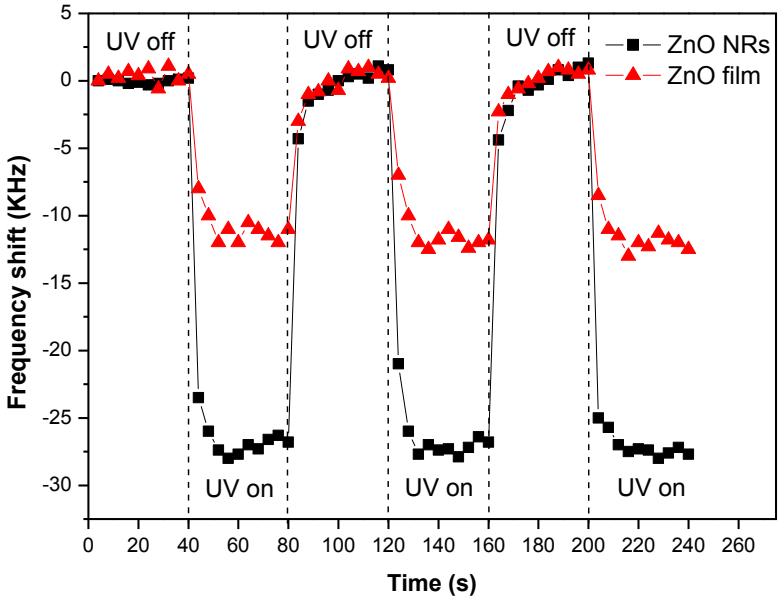
Frequency shift (KHz)
Time (s)
UV off
UV on
ZnO NRs
ZnO film

(d)

Figure 4.

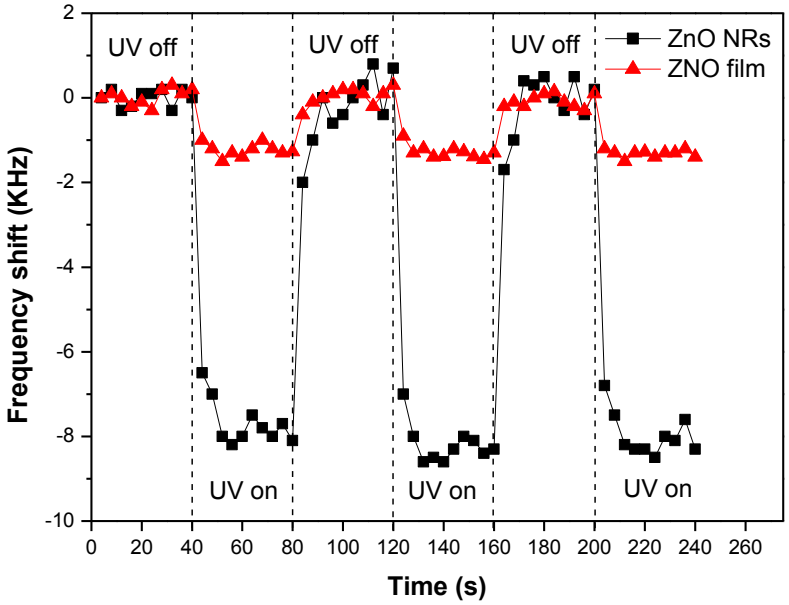
UV off
UV off
UV off
UV on
UV on
UV on
ZnO NRs
ZNO film
Frequency shift (KHz)
Time (s)
2
0
-2
-4
-6
-8
-10
0
20
40
60
80
100
120
140
160
180
200
220
240
260

Figure 5.